Study of hot electrons in AlGaN/GaN HEMTs under RF Class B and Class J operation using electroluminescence

Tommaso Brazzini [a,*], Michael A. Casbon [b], Huarui Sun [a], Michael J. Uren [a], Jonathan Lees [b], Paul J. Tasker [b], Helmut Jung [c], Hervé Blanck [c], Martin Kuball [a]

[a] Center for Device Thermography and Reliability, H. H. Wills Physics Laboratory, University of Bristol, Bristol BS8 1TL, United Kingdom
[b] Centre for High Frequency Engineering, Cardiff University, Cardiff, CF24 3QR, United Kingdom
[c] United Monolithic Semiconductors GmbH, Wilhelm-Runge-Strasse 11, 89081 Ulm, Germany

ARTICLE INFO

ABSTRACT

Electroluminescence microscopy and spectroscopy have been used to investigate hot electron concentration and electron temperature during RF operation. Two modes of operation were chosen, Class B and Class J, and compared with DC conditions. Hot electron concentration and temperature were on average lower for both RF modes than under comparative DC conditions. While these average values suggest that degradation due exclusively to hot electrons may be lower for RF than for DC conditions, the peak values in EL intensity and electric field along dynamic load lines have also to be taken into account and these are higher under Class J than Class B.

© 2015 The Authors. Published by Elsevier Ltd. This is an open access article under the CC BY license (http://creativecommons.org/licenses/by/4.0/).

1. Introduction

AlGaN/GaN high-electron-mobility transistors (HEMTs) offer a very promising solution to the increasing demand for high power switches and radio frequency (RF) power amplifiers. The GaN large band gap, high breakdown field and saturation velocity make this material well suited for high power operation from microwave to millimeter wave frequencies. However, GaN based devices still face some reliability issues when operating conditions are pushed to the extremes. For example, reliability under RF operation is still not fully resolved, and works among groups are still in progress for the complete understanding of this issue [1–6].

Gate metal instabilities [4] and inverse piezoelectric effects [5] have been identified as sources of early device failure after accelerated RF life tests for different applied frequencies (X-band or L-band). Some correlation has been observed between the increase in drain-to-source on-state resistance and output power degradation, most likely due to an increased surface charge between the gate and drain [2]. RF degradation tests are expensive to perform and not always trivial to interpret [1], hence pulsed I-V signal configuration and DC lifetime testing are often used as alternatives [4]. However it is not fully clear how reliable DC

testing is in assessing RF degradation, as failure mechanisms can be different in the two cases. Some groups have reported increased RF degradation compared to DC lifetime testing [3] while according to other studies, RF and DC excitations show the same degree of degradation [7,8]. Hot carriers have been suggested to be responsible for generating traps in the gate-drain access region and, due to negative charge injection, for the increase in access resistance values observed [3,9].

Electroluminescence (EL) imaging and spectroscopy have been shown in the past to be efficient tools for monitoring hot electron concentrations and energy during operation [6,10,11,12] as well as for assessment of device degradation after test. EL intensity has been reported to be correlated with degradation under DC conditions [13,14], which has been suggested to be due to high energy carriers modifying defect states or creating new defects inside the device epilayers [15]. The direct observation of hot electrons during RF has been recently reported during Class B operation [6]. It was shown that hot electron density under Class B operation is lower, on average, than under comparable DC operation. Also, hot electrons under RF device operation exhibited a lower average electron temperature compared to DC, by up to 500 K. The results suggested that potential hot electron degradation mechanisms under Class B mode could be lower than under DC if no other degradation mechanisms were present (e.g. field-driven degradation).

In the present work, this earlier method is extended to the understanding and comparison of hot electrons under Class B and Class J

* Corresponding author.
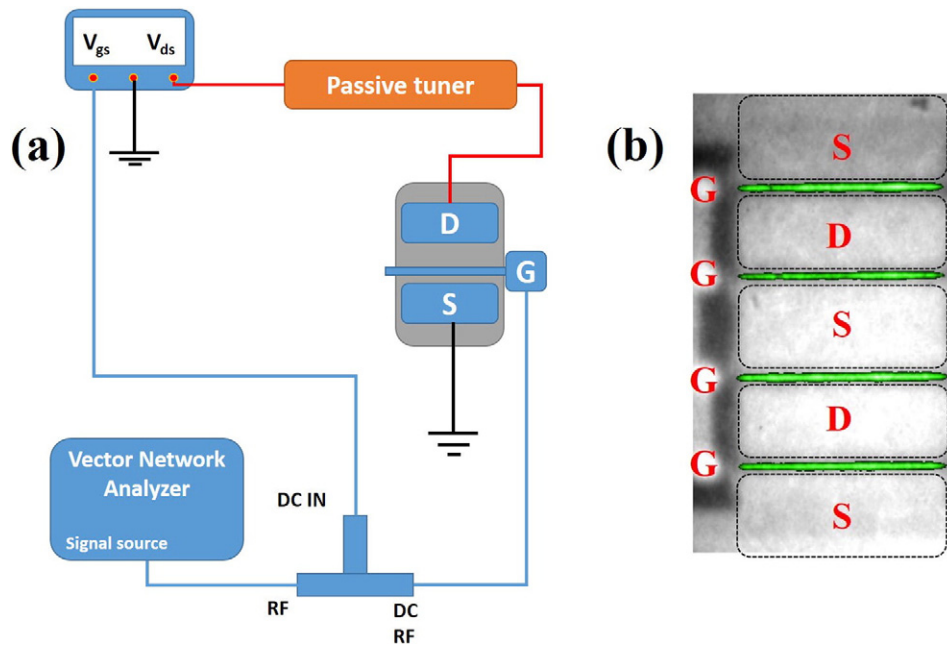E-mail address: tommaso.brazzini@bristol.ac.uk (T. Brazzini).

Fig. 1. (a) Schematic of the circuit used for the measurements. (b) False-color EL image of AlGaN/GaN HEMT, overlaid on a white-light image for a 4×100 µm-wide device. The device was operated under DC $V_{DS} = 20$ V and $V_{GS} = -3$ V.

modes of operation of AlGaN/GaN HEMTs using EL microscopy and spectroscopy. Class B is a standard mode used in RF power amplifier design offering high efficiency while amplifying only half of the input wave cycle. The Class J mode has shown the potential of obtaining the same efficiency and output power, but without requiring a band-limiting second harmonic short circuit termination [16]. The comparative analysis in terms of hot electrons of these two modes, which represent two extremes on a continuum of modes having different maximum drain voltage swings, but which cannot easily be distinguished by simple RF performance measurements, is important in assessing the vulnerability of power amplifiers to degradation.

2. Experimental details

The 4×100 µm HEMTs studied here were AlGaN/GaN heterostructures with a Fe-doped GaN buffer layer on a semi-insulating SiC substrate, with a 0.25 µm gate length. During testing, the devices were operated in specific RF operating modes, Class B and Class J, using a matching section circuit (passive tuner), built following active load-pull characterization of the devices. A 1 GHz signal was applied to the gate of the device using a vector network analyzer (VNA) (see Fig. 1(a) for the schematic of the setup). An average DC drain current was measured for each fixed input RF power. Class B operation involves applying a resistive load at the fundamental frequency and a short circuit to higher harmonics, and was selected since it is commonly used for delivering high power added efficiency (PAE). The result is a nominally sinusoidal voltage and a half wave rectified current waveform, which only flows while the voltage is at a minimum, therefore minimizing dissipation and maximizing PAE. The Class J mode is a variant of Class B which can also deliver efficient wideband amplifier operation [16,17]. In Class J, the current waveform and hence the quiescent DC bias state are unchanged. The voltage waveform is however modified, becoming half wave rectified, by the introduction of reactive terminations at both the fundamental and second harmonic, such that the RF output power and PAE is also unchanged. The really significant difference between these modes is that the output voltage waveform has much higher peak for Class J than Class B. For each operating mode the dynamic current–voltage locus was varied by changing input RF

power. The same bias point was used for both operating modes. An optical microscope, with a $50 \times$ objective, was used for EL light detection, from the backside of the device allowing collection of the emission from the whole operating region under metal contacts. A Hamamatsu CCD camera was used for EL microscopy, while a Renishaw InVia spectrometer was used for spectral acquisition. During operation, the device temperature was monitored with micro-Raman thermography. Further details on this technique can be found in Ref [18].
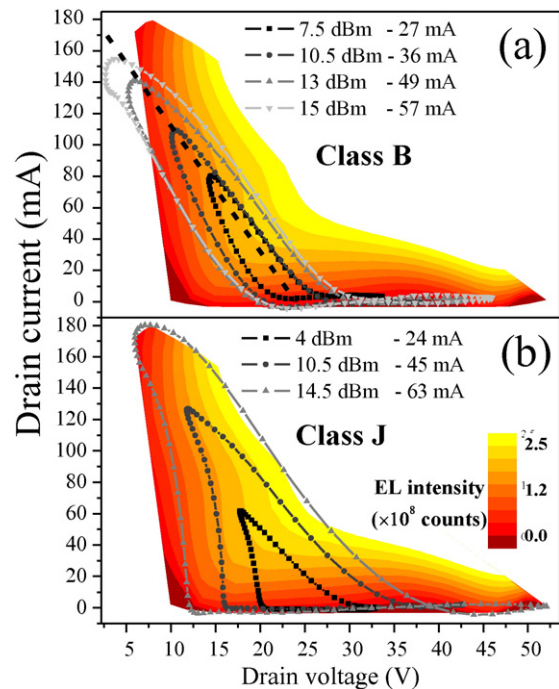

Fig. 2. Contour maps of the EL intensity in I_{DS}-V_{DS} plane, obtained under DC conditions. Superimposed are the load lines for Class B (a) and Class J (b) used for EL experiments at the indicated input RF power levels and drain currents. In the top part the 125 Ω DC load line used for comparisons is also shown (short dash).
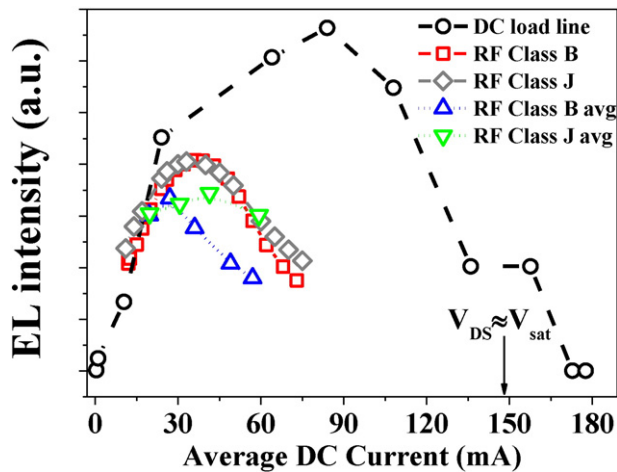
Fig. 3. Dependence of the EL intensity on the average current for DC (black circles) along the load line, and for RF Class B (red squares) and RF Class J (gray diamonds) operation as RF input power is varied. Triangles are EL intensity values obtained through averaging the RF load line using the DC measured EL intensity values as shown in Fig. 4. The lines are guides to the eye.

3. Results and discussions

For a first estimation of the hot electron density in AlGaN/GaN HEMTs under RF operation, the load lines for the two modes of operation, Class B and J, for different RF powers, have been superimposed onto an EL contour map obtained at different bias points under static DC operation as shown in Fig. 2. Maximum EL intensity can be observed when the load line passes through the semi-on region when the product of current and voltage is the highest at the output which is consistent with previous reports [12,19]. A DC load line with resistance $R_L = 125$ Ω was used as a comparison and was chosen to track the on-part of the Class B load lines. For both modes of operation the quiescent bias point was chosen to be $V_{DS} = 24$ V and $V_{GS} = -3.7$ V.

The results of the EL measurements are reported in Fig. 3, showing EL intensity as a function of average DC current. For DC, the gate voltage is varied to follow the load line and for RF the input RF power is varied at fixed gate bias. The EL intensity obtained under RF operation for both modes is compared to the EL intensity measured under DC. The EL intensity is measured as an average over many cycles of 1 ns each over the full load line, as the integration time of the CCD camera was fixed at 50 ms. The input power under RF drive was varied between -10 dBm and $+15$ dBm, corresponding to a DC average current between 11 mA and 75 mA. From these results we can conclude that on a similar load line, the hot electron contributions during operation are higher under DC compared to RF, consistent with our earlier data [6]. Despite the marked difference in the load-line cycles of Class J and Class B, EL measurements under the two modes of operation appear remarkably similar in terms of intensity and shape. The 'semi-on' parts of the load line determine predominantly the average EL intensity; for RF cases the load line passes through similar regions where the hot electron contribution is higher (see Fig. 2).

To enable a more detailed comparison between DC, Class B and Class J device operations, an average of the EL intensity was obtained over the load lines used during the measurements. The EL variation along the load line was extracted from the EL intensity contour map of Fig. 2, with the result shown in Fig. 4. It is then possible to average the EL intensity measured over an entire cycle under RF for each average DC current. This gives reasonable agreement with the measured values as shown in Fig. 3. This fact makes the EL measurements a powerful tool for predictions of hot electron contributions during operation. The slight difference between measured and predicted EL intensity can be ascribed to difference in self-heating effects between RF and DC. Temperature effects on the degradation under RF have not been included in the present study [20].

In terms of degradation predictions of Class J and Class B RF versus DC operation, the impact of hot electrons appears to be potentially less strong on average during RF device operation compared to a similar DC condition, considering a comparable load line, and only considering the average hot electron density. However, there are maxima in the EL intensity and therefore hot electron concentration and these will have impact on device degradation. This is why the dynamic profiles shown
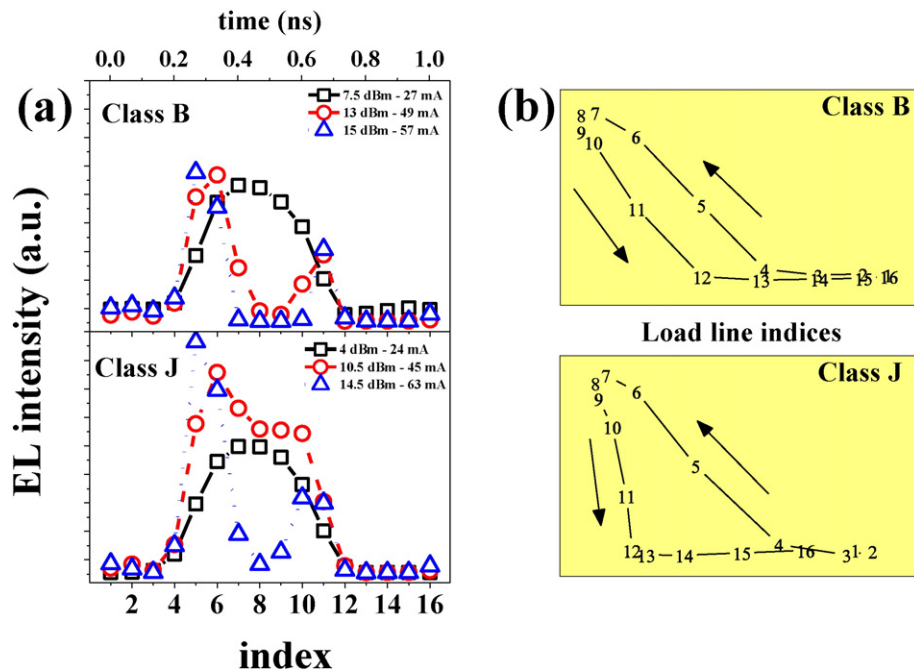

Fig. 4. (a) EL intensity along the load lines for Class B and Class J. For comparison the Y-axis has the same range for the two cases; (b) indicates the load-line indices for Class B and Class J device operations.
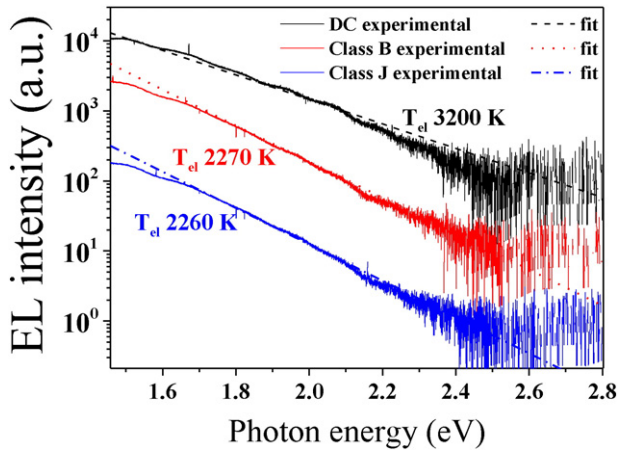
Fig. 5. Electroluminescence spectra under DC and RF Class B and Class J operation for the same average DC current (20 mA). The spectra have been vertically shifted for clarity. The results of the fitting are also shown.

in Fig. 4 are important for the prediction of hot electron degradation behavior. Even though the two RF modes show a similar average EL intensity, Class J exhibits an increased EL signal peak compared to Class B at high input power. This suggests that under similar input signal there should be a higher impact of hot electron induced degradation under Class J compared to Class B device operation, with the difference increasing with higher input power.

From a device reliability point of view, not only the density of hot carriers but also the electron energy is a very important parameter. This is because there is a threshold energy to create trap centers by hot carriers [15], which then potentially degrade device performance. Hence a method for the estimation of carrier energy is required to predict the amount of degradation in an electronic device. Light emission from a device can be resolved spectroscopically showing an emission band extending over the visible and infrared spectral range [21,22,23,24]; intra-band mechanisms, such as Bremsstrahlung, have been suggested to be responsible for the observed spectrum [12,23,24]. Under the assumption of Maxwell–Boltzmann distribution of the electrons, the high energy part of the emission spectrum can be approximated with a simple exponential form such as [23]:

$$I_{EL}(E) \sim \exp\left(-\frac{E}{k_B(T_{el} - T_{latt})}\right) \quad (1)$$

where the dependence of the EL intensity (I_{EL}) on the photon energy (E) is strongly influenced by both lattice temperature (T_{latt}) and electron temperature (T_{el}). In most practical cases, the electron temperature is much higher than the lattice temperature [21], and this case can be neglected. In our case, the lattice temperature rise was estimated by means of Raman thermography and found to be at most 30°C in the range of currents used during both RF and DC operation. Electron temperatures, as fitting parameters, were extracted with Eq. (1), as shown in Fig. 5, from the experimental data. In the spectra, interference fringes are visible and are due to the internal reflection at the GaN interfaces. The comparison of DC and RF electron temperature is displayed in Fig. 6(b); Fig. 6(a) illustrates spectra and electron temperature obtained under DC. The load line used for spectral measurements is the same as the one used for EL intensity measurements.

The electron temperatures measured under both RF modes, representing the average electron temperature over a 1 ns-cycle of the load line, are lower than the DC measured electron temperature by up to 500 K and decreases with increasing RF input power. The reason can be understood by considering Fig. 7 illustrating the electron temperature contour map. Overlapped in Fig. 7 are the DC points of the measurements (a) and the Class J load lines (b). For DC, electron temperature decreases with increasing DC current going from a lower current and high electric field to a high current and low electric field. Since the semi-on parts of the load lines have the highest EL intensity (see Fig. 2), the measured EL spectrum under RF (as illustrated in Fig. 5) is mostly dominated by these semi-on regions. Therefore, for RF the determined electron temperature corresponds to what would be measured in the red part of the load lines highlighted in Fig. 7(b) [6]. With increasing input power, the red parts will shift to points on the load lines with a lower electron temperature, which is consistent with the values experimentally measured. The case of Class B is analogous. Moreover, these devices show DC-RF dispersion (current-collapse) associated with surface trapping [25]. This furthermore induces a reduction in the measured electron temperature as the electric field decreases, as already previously reported [6,26].

Despite the marked differences of the load-line cycles between the two modes (higher maximum V_{DS} voltage for Class J and lower V_{GS} for Class B because of rectification), the average hot electron contribution comes out to be very similar. To explain this, it is important to consider that at relatively low input power, as in the present work, the main contributions come from the semi-on part, which is in a similar region in the two modes. Possibly, an increase in the input power would enhance the differences, either in terms of EL intensity or electron temperature, and as a consequence it is likely that also the degradation would be different in the two cases.
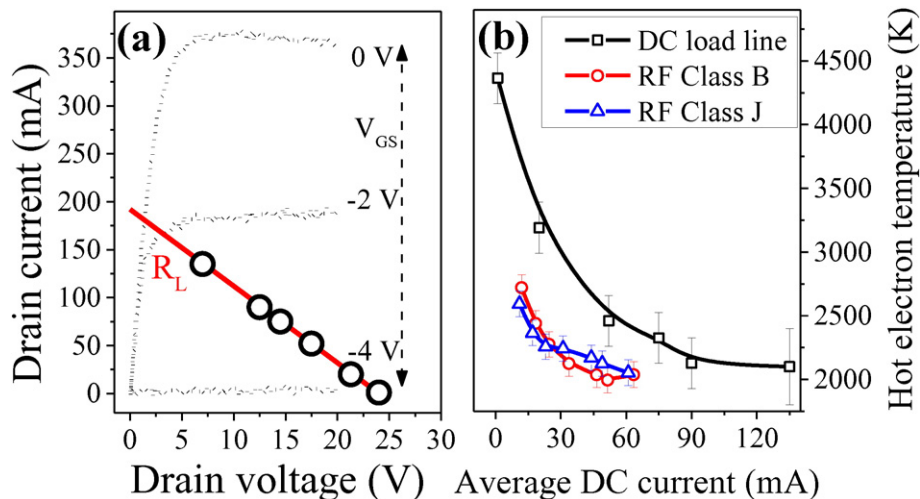

Fig. 6. (a) I_{DS}-V_{DS} device characteristic and DC load line used for spectral emission measurements under DC conditions. The circles are the points at which the electron temperature was measured. (b) Comparison of the electron temperatures obtained under RF Class B and J as well as DC as a function of average drain current. Lines are a guide to the eye.
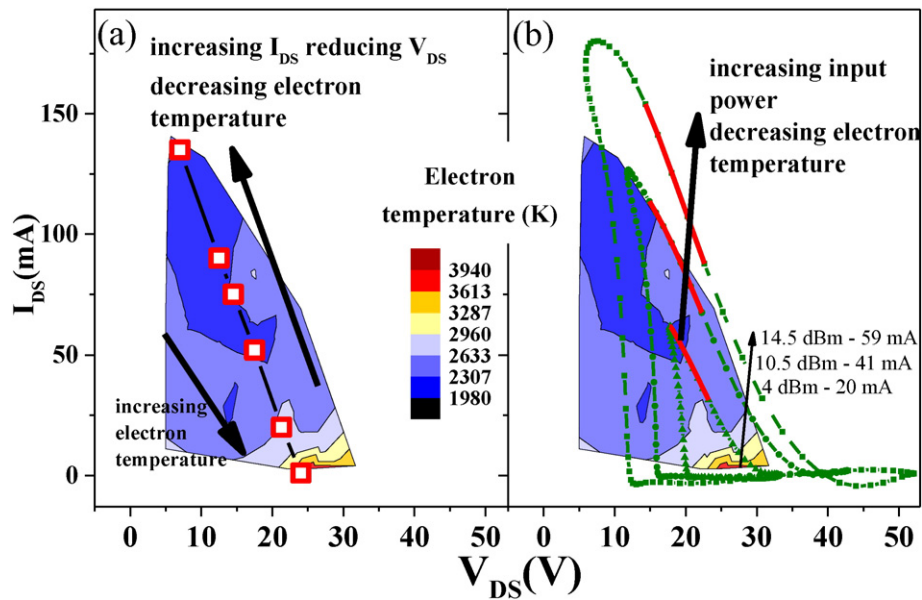
Fig. 7. Electron temperature in DC (a) and RF Class J (b). In (a) the red squares are the points at which the electron temperature was measured. The highest electron temperature is found at high V_{DS} and low I_{DS}, as shown in the map. In (b) under RF the peak EL intensity regions for each RF power are highlighted with red lines on the load lines. The higher the power input (current), the lower the electron temperature.

A lower average electron temperature under RF operation is observed, and this could suggest a reduced impact of hot carriers under RF excitation with respect to DC on device degradation. However, peak electron temperature rather than just average value need to be considered during the cycle over the load line, similar to the earlier discussion of EL intensity. Referring to Fig. 8(a), during the load-line cycle, there are points at which the EL intensity is very low (i.e. high V_{DS} and low I_{DS}). At those points the EL intensity is small but a very high electric field is present, i.e. a very high hot electron temperature (Fig. 8(b)). Due to the low EL signal, these high electric field points will not be detected in the EL spectrum during RF operation, which averages over the entire load line. This fact complicates the prediction of whether RF or DC device degradation is more severe, however there are certain differences which need to be considered in the hot electron distribution which are often ignored. Here the main points of the present study are summarized:

1. Regarding EL intensity i.e. hot electron density,
a. While under RF on average the values are lower compared to DC, the intensity reaches high peak values. These are the points where the

load line passes through the semi-on condition, where hot electron degradation is most likely to occur. If this instantaneous intensity exceeded the DC values, then that could induce a higher, or at least equal, hot electron degradation than DC.
b. Class J could potentially be more severe in hot carrier degradation than Class B as peak EL intensity values are higher.
2. Regarding hot electron temperature,
a. Although on average the values extracted are lower under RF than under DC for the same current, in each RF cycle near the off-state at high V_{DS}, the hot electron temperature is higher than under DC conditions. Although the number of hot carriers under this condition is very low (with the current near zero), they are likely to be more capable of causing damage. In terms of device degradation, although considering average electron temperature one may expect lower hot electron degradation under RF, if degradation due to electric fields (high V_{DS}, low V) is present, then EL is not a good reliability indicator.
b. Class J operation could be more affected by high V_{DS} and low V_{GS} points compared to Class B for the same input power, as its maximum V_{DS} is higher.
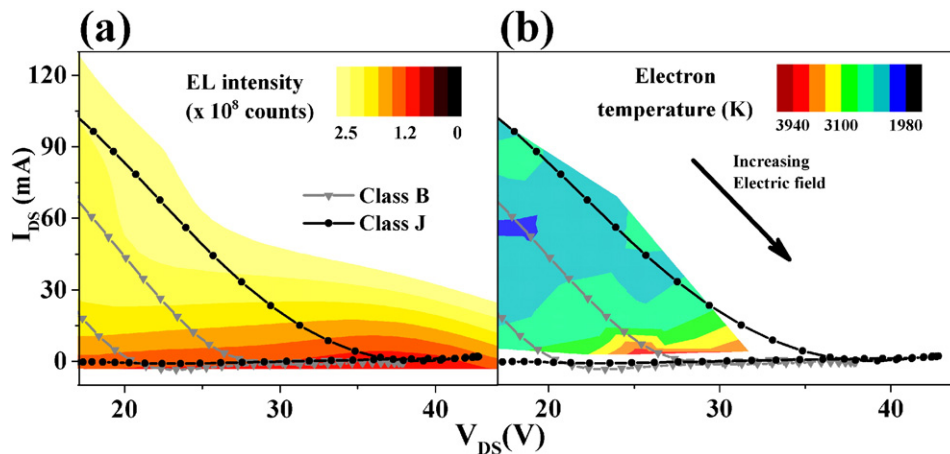

Fig. 8. Expanded view of the high-voltage contour maps. (a) EL intensity map contour map, with Class B and Class J load line (10 dBm input power) superimposed. (b) The same load lines are superimposed on the electron temperature map. Both maps obtained under DC conditions.

4. Conclusions

Hot electron behavior in two relevant modes of RF operation (Class B and Class J) has been analyzed in AlGaN/GaN HEMTs and compared to DC device operation on a similar load line. On average, both RF modes showed a reduced hot electron concentration and electron energies (electron temperatures), however, they showed high peak values, especially under Class J. Correspondingly the spectral measurements show that the average electron temperature during RF is lower than under DC conditions, however high peak electron temperature values on sub-nanosecond timescales are present, and are again more significant in the Class J case. This study indicates that EL is a valuable tool for assessing hot carrier dynamics, but cannot be used directly as an indicator of device vulnerability to hot carrier degradation.

Acknowledgments

References

[1] A. Sozza, C. Dua, E. Morvan, B. Grimber, S.L. Delage, A 3000 hours DC life test on AlGaN/GaN HEMT for RF and microwave applications, Microelectron. Reliab. 45 (2005) 1617, http://dx.doi.org/10.1016/j.microrel.2005.07.081.

[2] A.M. Conway, M. Chen, P. Hashimoto, P.J. Willadsen, M. Micovic, Accelerated RF life testing of GaN HFETs, IEEE 07CH37867 45th Annual international Reliability Physics Symposium, Phoenix 2007, pp. 472–475, http://dx.doi.org/10.1109/RELPHY.2007.369936.

[3] J. Joh, J.A. Del Alamo, RF power degradation of GaN high electron mobility transistors, IEDM Technical Digest Dec. 2010, p. 20.2.1, http://dx.doi.org/10.1109/IEDM.2010.5703397.

[4] J.-B. Fonder, O. Latry, C. Duperrier, M. Stanislawiak, H. Maanane, P. Eudeline, F. Temcamani, Compared deep class-AB and class-B ageing on AlGaN/GaN HEMT in S-band pulsed-RF operating life, Microelectron. Reliab. 52 (2012) 2561, http://dx.doi.org/10.1016/j.microrel.2012.04.024.

[5] A.R. Barnes, F. Vitobello, preliminary reliability data from accelerated RF life tests on European GaN HEMTs, CS MANTECH Conference Boston, Massachusetts, USA April 23rd - 26th, 2012, pp. 87–90.

[6] T. Brazzini, M.A. Casbon, H. Sun, M.J. Uren, J. Lees, P.J. Tasker, H. Jung, H. Blanck, M. Kuball, Electroluminescence of hot electrons in AlGaN/GaN high-electron-mobility transistors under radio frequency operation, Appl. Phys. Lett. 106 (2015) 213502, http://dx.doi.org/10.1063/1.4921848.

[7] M. Caesar, M. Dammann, V. Polyakov, P. Waltereit, W. Bronner, M. Baeumler, R. Quay, M. Mikulla, O. Ambacher, Generation of traps in AlGaN/GaN HEMTs during RF-and DC-stress test, IEEE IRPS April 2012, p. CD.6.1, http://dx.doi.org/10.1109/IRPS.2012.6241883.

[8] P. Valizadeh, D. Pavlidis, Effects of RF and DC stress on AlGaN/GaN MODFETs: a low-frequency noise-based investigation, IEEE Trans. Device Mater. Reliab. 5 (2005) 555, http://dx.doi.org/10.1109/TDMR.2005.853515.

[9] A. Chini, V. Di Lecce, F. Fantini, G. Meneghesso, E. Zanoni, Analysis of GaN HEMT failure mechanisms during DC and large-signal RF operation, IEEE Trans. Electron Devices 59 (2012) 1385, http://dx.doi.org/10.1109/TED.2012.2188636.

[10] M. Montes Bajo, C. Hodges, M.J. Uren, M. Kuball, On the link between electroluminescence, gate current leakage, and surface defects in AlGaN/GaN high electron mobility transistors upon off-state stress, Appl. Phys. Lett. 101 (2012) 033508, http://dx.doi.org/10.1063/1.4737904.

[11] H. Sun, M. Montes Bajo, M.J. Uren, M. Kuball, Implications of gate-edge electric field in AlGaN/GaN high-electron-mobility transistors during off-state degradation, Microelectron. Reliab. 54 (2014) 2650, http://dx.doi.org/10.1016/j.microrel.2014.09.020.

[12] G. Meneghesso, G. Verzellesi, F. Danesin, F. Rampazzo, F. Zanon, A. Tazzoli, M. Meneghini, E. Zanoni, Reliability of GaN high-electron-mobility transistors: state of the art and perspectives, IEEE Trans. Device Mater. Reliab. 8 (2008) 332, http://dx.doi.org/10.1109/TDMR.2008.923743.

[13] M. Meneghini, A. Stocco, R. Silvestri, G. Meneghesso, E. Zanoni, Degradation of AlGaN/GaN high electron mobility transistors related to hot electrons, Appl. Phys. Lett. 100 (2012) 233508, http://dx.doi.org/10.1063/1.4723848.

[14] M. Dammann, M. Baeumler, F. Gütle, M. Cäsar, H. Walcher, P. Waltereit, W. Bronner, S. Müller, R. Kiefer, R. Quay, R. Mikulla, O. Ambacher, A. Graff, F. Altmann, M. Simon, Reliability and degradation mechanism of 0.25 μm AlGaN/GaN HEMTs under RF stress conditions, Integrated Reliability Workshop Final Report (IRW) October 16th-20th 2011, pp. 42–46, http://dx.doi.org/10.1109/IIRW.2011.6142585.

[15] Y.S. Puzyrev, B.R. Tuttle, R.D. Schrimpf, D.M. Fleetwood, S.T. Pantelides, Theory of hot-carrier-induced phenomena in GaN high-electron-mobility transistors, Appl. Phys. Lett. 96 (2010) 053505, http://dx.doi.org/10.1063/1.3293008.

[16] P. Wright, J. Lees, P.J. Tasker, J. Benedikt, S.C. Cripps, An efficient, linear, broadband class-J-mode PA realised using RF waveform engineering, IEEE MTT-S Int. Microwave Symp. Digest June 2009, pp. 653–656, http://dx.doi.org/10.1109/MWSYM.2009.5165781.

[17] S. Preis, D. Gruner, G. Boeck, Investigation of class-B/J continuous modes in broadband GaN power amplifiers, IEEE MTT-S International Microwave Symposium, Montreal, Canada 17th-22nd June 2012, pp. 1–3, http://dx.doi.org/10.1109/MWSYM.2012.6258413.

[18] J.W. Pomeroy, M. Kuball, D.J. Wallis, A.M. Keir, K.P. Hilton, R.S. Balmer, M.J. Uren, T. Martin, P.J. Heard, Thermal mapping of defects in AlGaN/GaN heterostructure field-effect transistors using micro-Raman spectroscopy, Appl. Phys. Lett. 87 (2005) 103508, http://dx.doi.org/10.1063/1.2041823.

[19] M. Meneghini, G. Meneghesso, E. Zanoni, Analysis of the reliability of AlGaN/GaN HEMTs submitted to on-state stress based on electroluminescence investigation, IEEE Trans. Device Mater. Reliab. 13 (2013) 357, http://dx.doi.org/10.1109/TDMR.2013.2257783.

[20] J.W. Pomeroy, M.J. Uren, M. Kuball, B. Lambert, GaN HEMT channel temperature in accelerated life testing: RF versus DC, ROCS Workshop, Reliability of Compound Semiconductors Workshop, Scottsdale, Arizona, May 18 2015 2015, pp. 77–79.

[21] A. Toriumi, M. Yoshimi, M. Iwase, Y. Akiyama, K. Taniguchi, A study of photon emission from n-channel MOSFET's, IEEE Trans. Electron Devices ED-34 (1987) 1501, http://dx.doi.org/10.1109/T-ED.1987.23112.

[22] H.P. Zappe, "Hot-electron electroluminescence in GaAs transistors", Semicond. Sci. Technol. 7 (1992) 391, http://dx.doi.org/10.1088/0268–1242/7/3/020.

[23] N. Shigekawa, K. Shiojima, T. Suemitsu, Optical study of high-biased AlGaN/GaN high-electron-mobility transistors, J. Appl. Phys. 92 (2002) 531, http://dx.doi.org/10.1063/1.1481973.

[24] J.W. Pomeroy, M. Kuball, M.J. Uren, K.P. Hilton, R.S. Balmer, T. Martin, Insights into electroluminescent emission from AlGaN GaN field effect transistors using micro-Raman thermal analysis, Appl. Phys. Lett. 88 (2006) 023507, http://dx.doi.org/10.1063/1.2163076.

[25] C. Roff, J. Benedikt, P.J. Tasker, D.J. Wallis, K.P. Hilton, J.O. Maclean, D.G. Hayes, M.J. Uren, T. Martin, Analysis of DC-RF dispersion in AlGaN/GaN HFETs using RF waveform engineering, IEEE Trans. Electron Devices 56 (2009) 13, http://dx.doi.org/10.1109/TED.2008.2008674.

[26] S. Ohi, Y. Sakaida, J.T. Asubar, H. Tokuda, M. Kuzuhara, Correlation between electroluminescence and current collapse in AlGaN/GaN HEMTs, CS MANTECH Conference, Scottsdale, Arizona USA May 18th - 21st, 2015, pp. 265–268.